Experimental study of bound and autoionizing Rydberg states of the europium atom*

Xiao Ying(肖 颖), Dai Chang-Jian(戴长建)†, and Qin Wen-Jie(秦文杰)

School of Science, Tianjin University of Technology, Tianjin 300384, *China*

(Received 19 June 2009; revised manuscript received 13 November 2009)

An isolated-core-excitation (ICE) scheme and stepwise excitation are employed to study the highly excited states of the europium atom. The bound europium spectrum with odd parity in a region of 42400–43500 cm^{-1} is measured, from which spectral information on 38 transitions, such as level position and relative intensity, can be deduced. Combined with information about excitation calibration and the error estimation process, the selection rules enable us to determine the possible values of total angular momentum J for the observed states. The autoionization spectra of atomic europium, belonging to the $4f^7 6pnl$ ($l = 0, 2$) configurations, are systematically investigated by using the three-step laser resonance ionization spectroscopy (RIS) approach. With the ICE scheme, all the experimental spectra of the autoionizing states have nearly symmetric profiles whose peak positions and widths can be easily obtained. A comparison between our results and those from the relevant literature shows that our work not only confirms many reported states, but also discovers 14 bound states and 16 autoionizing states.

Keywords: europium atom, isolated-core-excitation, highly excited states, autoionizing Rydberg states

PACC: 3280, 3270

1. Introduction

In the past decades, studies on highly excited atoms have been advanced dramatically with the development of the laser. In particular, the investigation of atomic autoionizing states has recently received a lot of attention because it is related to many interesting phenomena, such as propagation without absorption[1] and coherent control.[2] In spite of numerous applications, information on the autoionizing states of rare-earth atoms[3−5] is still scanty. Among the rare-earth atoms, the Yb atom has been studied most[6,7] due to the fact that the 4f shell is completely filled. With only two s-electrons outside the closed shell, the spectrum of the Yb atom is basically an alkaline-earth-like spectrum. However, with a half-filled 4f shell, the Eu atom is very active and thus has a much more complex nature in its spectra. Therefore, only a few studies on the Eu atom have been reported.[8] Although some work on the Eu atom has been done, it is limited only in some regions or with some excitation schemes. For example, the odd-parity bound states[9] have been reported only in an energy range from 45000 cm^{-1} to 45735 cm^{-1}, while the autoionizing states[10] are obtained only with a two-step excitation scheme.

The ICE scheme, as a powerful experimental method, has several advantages. First, only low laser powers are required because all the transitions are single-electron transitions, thereby leading to the second advantage, i.e. a simplified autoionization spectrum, whose profile is determined only by configuration interaction rather than by a combination of configuration interaction and interference effects, from which information on the peak and width of a resonance can be easily obtained. Furthermore, unlike the case of a Fano profile, the peak position and the width of an observed spectrum with the ICE scheme can be interpreted as level energy and autoionization rate. Thus, the ICE scheme has been used extensively for investigating the autoionizing states of alkaline-earth atoms,[11] such as the Ba atom.[12−15] However, due to the much more complex nature of the Eu atom its Rydberg states are very different from those of alkaline-earth atoms. For instance, they are perturbed seriously by many valence states: when an electron is excited the rest of the electrons are certainly not in an isolated core any more. Thus, it is necessary and

*Project supported by the National Natural Science Foundation of China (Grant Nos. 10574098 and 10674102) and the Natural Science Foundation of Tianjin, China (Grant No. 05YFJMJC05200).

†Corresponding author. E-mail: cjdai@yahoo.com.cn

© 2010 Chinese Physical Society and IOP Publishing Ltd

important to check where the ICE scheme is still applicable to the autoionization spectra of the Eu atom. In other words, we should first attempt to use the ICE scheme to investigate the autoionizing states of atomic Eu, converging to the $4f^7 6p^+$ thresholds.

The rest of the present paper is organized as follows. The experimental approach is given in Section 2. The experimental results and discussion are presented in Section 3, and finally, the conclusions are given in Section 4.

2. Experiment

As the experimental setup and approach have been given in detail elsewhere,[16] only some basic principles will be outlined here. The experimental setup used in this work is illustrated in Fig. 1. It consists of three parts: a laser system, an atomic beam system and a data acquisition system. Three tunable dye lasers each with a width of 0.1 cm^{-1} are pumped by the second or third harmonics of a Giant-770 model Nd:YAG pulsed laser with a pulse duration of 6–8 ns running at 20 Hz. The Eu atom source is from an effusive atomic beam sprayed from a resistively heated oven in a vacuum chamber. The atomic beam is collimated and directed to a region between two electric field plates, 1 cm apart, where it is crossed perpendicularly by dye laser beams to avoid Doppler broadening. The data acquisition system, including a model 4121B boxcar and a 9650A digital pulse generator which are controlled by a computer, was purchased from AMETEC Company. In order to ensure the excitation sequence, the second and third laser pulses are delayed by 8–10 ns and 16–20 ns respectively with respect to that of the first laser, while the gate of the boxcar and the pulse of the electric field are also carefully controlled. After a time delay of 0.5 μs to the laser pulses, the ions, resulting from the excitation and subsequent decay of autoionizing states, are extracted by the pulsed electric field to an MCP detector, the output of which is fed into the boxcar and stored in a computer for further analysis.

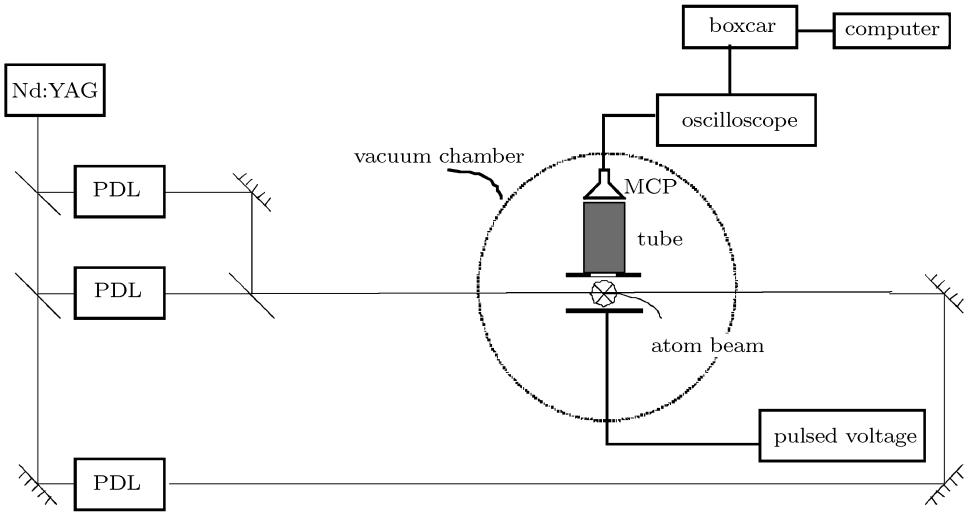


Fig. 1. Schematic diagram of the experimental apparatus including the excitation lasers (PDL: pulsed dye laser), the atomic beam, and the detection-analysis systems. The atomic beam is produced in the vacuum chamber. The ion signal is detected by an MCP, averaged by a boxcar, and stored in a computer for further analysis.

Figure 2(a) shows the scheme of two-colour stepwise excitation of the photoionization process. In order to fulfil the photoionization scheme, two linearly polarized lasers are employed to interact perpendicularly with the Eu atomic beam, which is extracted from the stainless steel oven. The first laser, fixed at a constant wavelength λ_1, excites the Eu atom to an intermediate state from its ground state. The second laser, whose wavelength λ_2 is scanned within a certain range, excites the atom to a highly excited state with an odd parity, and then ionizes it with another λ_2 photon. In order to make the experiment more fruitful, three photoionization schemes are employed:

(a) Scheme I

$$6s^2\ {}^8S_{7/2} \xrightarrow{\lambda_1=459.39\ \text{nm}} 6s6p\,{}^8P_{9/2} \xrightarrow{\lambda_2} [J = 7/2, 9/2, 11/2] \xrightarrow{\lambda_2} Eu^+; \quad (1)$$

(b) Scheme II

$$6s^2\ {}^8S_{7/2} \xrightarrow{\lambda_1=462.71\ \text{nm}} 6s6p{}^8P_{7/2} \xrightarrow{\lambda_2} [J = 5/2, 7/2, 9/2] \xrightarrow{\lambda_2} Eu^+; \tag{2}$$

(c) Scheme III

$$6s^2\ {}^8S_{7/2} \xrightarrow{\lambda_1=466.18\ \text{nm}} 6s6p{}^8P_{5/2} \xrightarrow{\lambda_2} [J = 3/2, 5/2, 7/2] \xrightarrow{\lambda_2} Eu^+. \tag{3}$$

A diagram of the ICE scheme and the relevant energy levels for the study of autoionizing states of the Eu atom are shown in Fig. 2(b). With the ICE scheme, the Eu atom is excited from the ground state $4f^76s^2$ to a $4f^76s6p$ state by the first dye laser. Then the atom is excited to a $4f^76snl$ ($l = 0$, 2) Rydberg state, whose outer nl ($l = 0$, 2) electron is in an orbit with a large radius, far from the Eu^+ $4f^76s^+$ core, by the second tunable dye laser. Finally, the atom is excited to an autoionizing state with the transition $4f^76s^+ \rightarrow 4f^76p^+$ by the third dye laser, thereby avoiding interference from the excitation of the nl electron. Due to considerable interaction with underlying continua converging to the $4f^76s^+$ or $4f^75d^+$ ionization limit, the atom in the $4f^76pnl$ ($l = 0$, 2) autoionizing state is very unstable, and decays quickly into an ion to the ionic states $4f^76s^+$ and $4f^75d^+$ by ejecting an electron.

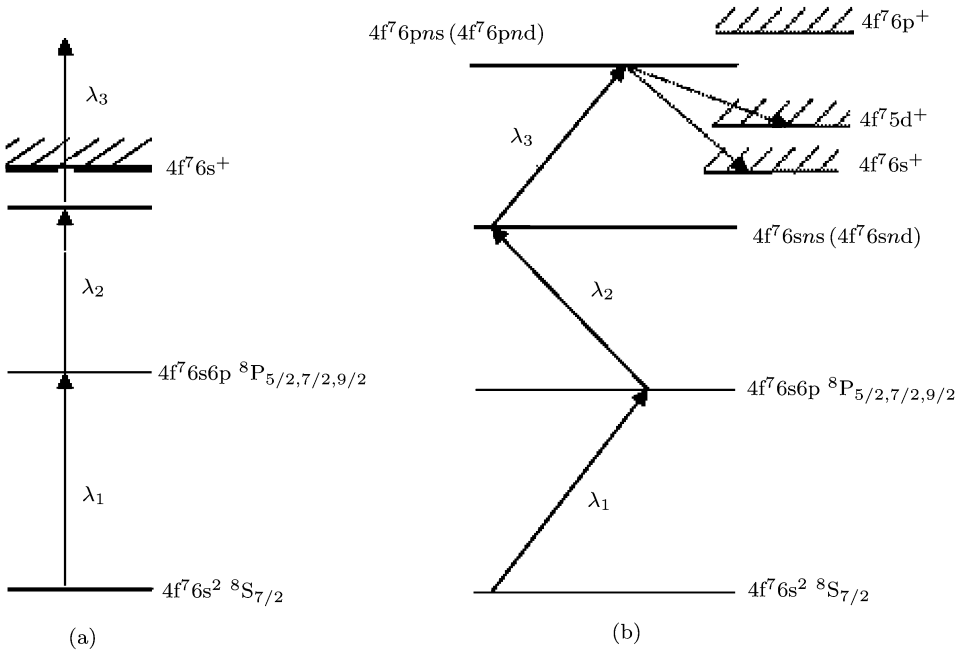


Fig. 2. Excitation schemes used in the experiment for the Eu atom. Panel (a) shows the photoionization process, where the wavelength of the first laser is fixed at the $4f^76s^2 \rightarrow 4f^76s6p$ resonance transition, while the wavelength of the second laser is scanned to excite the atoms into highly excited states. Panel (b) exhibits the autoionization process, where the wavelength of the first laser is fixed at the $4f^76s^2 \rightarrow 4f^76s6p$ resonance transition, and the wavelength of the second laser is fixed to excite the atoms into $4f^76snl$ ($l = 0$, 2) Rydberg states, then the wavelength of the third laser is scanned to excite the atoms into autoionizating states.

To ensure the accuracy of experimental data, both systematic and random errors are reduced carefully. For instance, the non-linearity in wavelength originating from the scanning system of dye lasers can be corrected by recording the interference spectrum of an F–P etalon, while a hollow cathode lamp is employed to calibrate the laser wavelength. On the other hand, as the power of the third laser is crucial to the width measurement of an autoionizing state, an effort is also made to eliminate power broadening in every autoionization spectrum. Specifically, the power of the third laser is reduced by using a suitable neutral-density filter until the ion signal decreases linearly as the laser power decreases. To reduce the random errors, we measure each spectrum several times and take the average of them. The uncertainty of the present experiment is estimated to be less than $\pm 0.20\ \text{cm}^{-1}$.

3. Results and discussion

In this section, many spectra of the bound and autoionizing states of the Eu atom are measured, from which a lot of experimental data are obtained with systematical analyses.

3.1. Highly excited bound states

As described in the previous section, three different intermediate states, $4f^7 6s6p\ ^8P_{5/2,7/2,9/2}$, are used to study the highly excited states of the Eu atom in the bound region, an example of which is shown in Fig. 3.

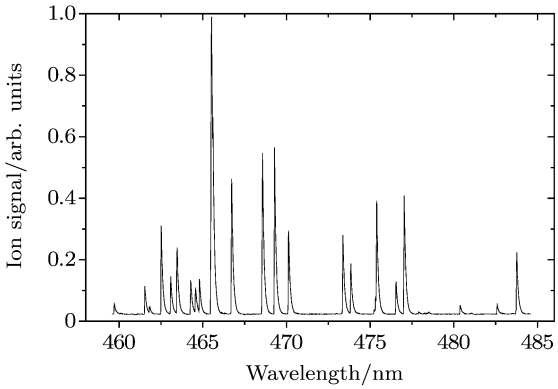


Fig. 3. Spectra of Eu atom using two-colour stepwise excitation and photoionization. The wavelength of second laser λ_2 is scanned from 460 nm to 485 nm, while the wavelength of the first laser λ_1 is fixed at 459.39 nm.

The wavelength λ_2 or photon energy E_2 of each peak of the above spectrum in Fig. 3 can be used to obtain the total energy of highly excited states from the relation $E = E_1 + E_2$, where E_1 denotes the photon energy of the first laser. All spectra from the two-colour stepwise photoionization are processed by this method to obtain precise data on the energy level, angular momentum and relative intensity. As shown in Table 1 the typical experimental uncertainty on level energy is estimated to be less than ± 0.20 cm^{-1}, and the relative intensities of the spectral lines are classified into three ranges: from 0 to 0.4, 0.4 to 0.7, and 0.7 to 1, marked with the symbols w, m and s respectively.

Compared with the previous work which uses a very different excitation scheme, the present experiment provides a great deal of information. Among the 38 transitions shown in Table 1, 14 have not been reported before, while the rest of them accord well with those reported in the literature in terms of energy.[17] Furthermore, the intensities of all observed spectral lines are also tabulated for the first time, providing some additional information about these states. For instance, the intensities of the newly discovered spectral lines are mostly weaker than those of transitions whose level energies have been reported before, which may partially explain why the previous work failed to observe them. Meanwhile, the above 14 weaker transitions indicate that their populations in these highly excited states are smaller than those of the rest listed in Table 1.

Table 1. Level energies, relative intensities, and the possible values of J of highly excited states of the Eu atom. Three excitation schemes are used to obtain the listed transition lines. The relative intensities are normalized and classified into three ranges: 0–0.4, 0.4–0.7, and 0.7–1, marked with the symbols w, m and s, respectively.

serial number	energy/cm^{-1}	excitation scheme	angular momentum (J)	intensity
1#	43423.2	I	7/2,9/2,11/2	w
2#	43410.6	I	7/2,9/2,11/2	w
3#	43378.3	I	7/2,9/2,11/2	w
4#	43350.7	I	7/2,9/2,11/2	w
5#	43343.4	II	5/2,7/2,9/2	w
6	43333.5	I, II	7/2,9/2	w
7#	43295.3	I, II	7/2,9/2	w
8	43281.7	I, II	7/2,9/2	w
9	43270.4	I	7/2,9/2,11/2	w
10	43238.5	I	7/2,9/2,11/2	s
11	43233.9	II	5/2,7/2,9/2	w
12	43184.2	I, II	7/2,9/2	m
13	43165.8	III	3/2,5/2,7/2	w
14	43100.9	I, II	7/2,9/2	m
15	43067.3	I, II	7/2,9/2	m
16	43030.1	I, II, III	7/2	w
17	42954.4	II	5/2,7/2,9/2	w
18	42937.6	II III	5/2,7/2	w
19#	42911.2	II	5/2,7/2,9/2	w
20	42895.8	III	3/2,5/2,7/2	w
21	42882.2	I, II	7/2,9/2	w
22#	42872.7	II	5/2,7/2,9/2	s
23	42860.9	I, II	7/2,9/2	w
24	42848.3	II	5/2,7/2,9/2	s
25#	42800.1	II	5/2,7/2,9/2	w
26#	42796.5	I	7/2,9/2,11/2	m
27#	42743.2	I, II	7/2,9/2	w
28#	42721.3	I, II	7/2,9/2	m
29	42697.2	II III	5/2,7/2	w
30	42682.5	II III	5/2,7/2	m
31	42575.5	I, II	7/2,9/2	w
32	42558.4	II III	5/2,7/2	s
33	42525.1	II III	5/2,7/2	m
34	42478.7	I, II	7/2,9/2	m
35	42453.0	III	3/2,5/2,7/2	s
36	42428.6	I	7/2,9/2,11/2	w
37#	42402.8	III	3/2,5/2,7/2	s
38#	42390.6	III	3/2,5/2,7/2	w

newly discovered

On the other hand, as the experimental data shown in Table 1 are obtained from the three different excitation schemes, it is very meaningful to make a comparison with each other in order to obtain information on the possible values of J of all measured bound states. According to the selection rules corresponding to the three excitation schemes, one may deduce the possible values of J for the states detected. Namely, for scheme I, we should have $J = 7/2$, $9/2$, or $11/2$; for scheme II $J = 5/2$, $7/2$, or $9/2$ and for scheme III $J = 3/2$, $5/2$, or $7/2$. With these principles, the possible values of the angular momentum of any state can be determined, and they are listed in Table 1. For instance, the J value of No. 16 state at 43030.1 cm^{-1} can be uniquely determined to be 7/2 as it can be detected by excitation schemes I, II and III simultaneously. Similarly, the J value of No. 28 state at 42721.3 cm^1 should be 7/2 or 9/2, as it can be detected by excitation schemes I and II simultaneously. Therefore, comparisons of spectra from the three different excitation schemes in the same energy region can indeed determine the possible values of J of the observed states.

3.2. Autoionizing states $4f^7 6p nl$

With the ICE scheme described in Section 2, the spectra of Eu $4f^7 6p nl$ autoionizing states are measured by scanning the wavelength of the third laser across the $4f^7 6s^+ \rightarrow 4f^7 6p^+$ ionic line transitions while the first two lasers are set to populate different $4f^7 6s nl$ bound Rydberg states. Since the transition of Eu^+ $4f^7 6s^+ \rightarrow 4f^7 6p^+$ should dominate the direct photoionization process (e.g. the $4f^7 6s nl \rightarrow 4f^7 6s \varepsilon l'$ transition), and eliminate the possible interference between the above two excitation pathways, the nl electron should basically acts like a spectator in the process of third-step excitation. In other words, most observed profiles with the ICE are expected to be basically of Lorentzian type. In order to confirm the above speculation, all the observed spectra are fitted to Lorentzian profiles, two examples of which are presented here.

As shown in Fig. 4, the spectrum of a $4f^7 6p nl$ autoionizing state can be a single resonance and it is well represented by a single-Lorentzian profile. Meanwhile, an autoionizing state may also have a spectrum with a double-peak profile as shown in Fig. 5. In this case, the level energy and width of an autoionizing state can be obtained by fitting the spectrum to the sum of two Lorentzian profiles.

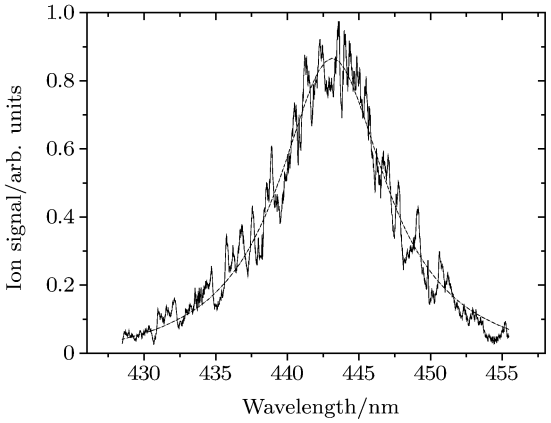


Fig. 4. Experimental autoionization spectrum of the Eu atom with a single peak. The spectrum represents the resonance transition by scanning λ_3 across the $4f^7 6s^+ J = 3 \rightarrow 4f^7 6p^+ J = 4$ ionic line in a range between 428.5 nm and 455.5 nm with λ_1 and λ_2 fixed at 466.18 nm and 573.81 nm respectively. The solid line represents the experimental spectrum, while the dash line is obtained from the Lorentzian fit.

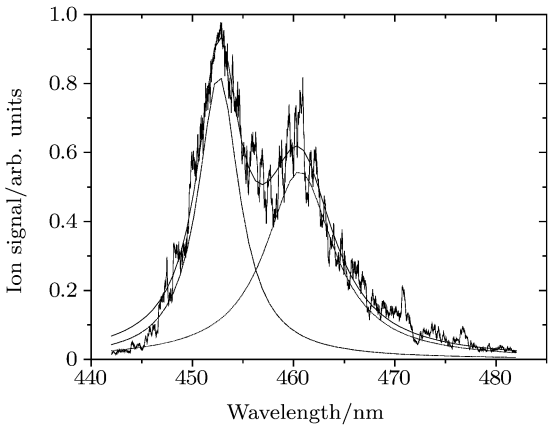


Fig. 5. Experimental autoionization spectrum of the Eu atom with a double-peak profile. It is obtained by scanning λ_3 from 442 nm to 482 nm, with λ_1 and λ_2 fixed at 462.71 nm and 565.84 nm, respectively. The solid line represents the experimental spectrum, while the dash line is obtained from the Lorentzian fit. The peak on the left represents the resonance transition at 22087.9 cm^{-1} when the wavelength of the third laser is scanned across the $4f^7 6s^+$ J=3$\rightarrow 4f^7 6p^+ J = 4$ ionic line; the one on the right represents the resonance transition at 21705.2 cm^{-1} when the wavelength of the third laser is scanned across the $4f^7 6s^+ J = 3 \rightarrow 4f^7 6p^+ J = 3$ ionic line.

Note that both λ_1 and λ_3 are different for Fig. 4 and Fig. 5. The peak on the left in Fig. 5 is centred at 22087.9 cm^{-1}, corresponding to the process in which λ_3 is scanned across the $4f^7 6s^+ J = 3 \rightarrow 4f^7 6p^+ J = 4$ ionic line, while the one on the right is centred at 21705.2 cm^{-1} corresponding to the process in which λ_3 is scanned across the $4f^7 6s^+ J = 3 \rightarrow 4f^7 6p^+ J = 3$ ionic line. Since the energy gap between the $4f^7 6p^+ J = 3$ and $J = 4$ ionization limits is

382.7 cm^{-1}, comparable to the widths of two autoionizing states converging to the two limits, they have a considerable overlap in energy, thereby leading to a double-peak profile.

Above all, taking advantage of the ICE method, the observed level energy and width of the Eu $4f^7 6pnl$ autoionizing state may be obtained by fitting its spectrum to either a single-peak or a double-peak Lorentzian profile as shown in Figs. 4 and 5, which is more accurate than reading them directly from the spectrum. On the other hand, these results not only confirm the speculation prior to the experiment, but also demonstrate that the ICE technique is applicable to more complex systems like the Eu atom.

With the above approach, the values of level energy E and width Γ of the $4f^7 6pnl$ autoionizing states can be tabulated. In a spectrum, the λ_3 value of a given peak gives its photon energy E_3 , and yields the energy of $4f^7 6pnl$ autoionizing states from the relation $E = E_1 + E_2 + E_3$ where E_1 and E_2 are the photon energies of the first and second lasers used. Note that the uncertainties in level energy E and width Γ are estimated to be less than ± 0.2 cm^{-1}.

Table 2. Autoionizing states converging to the $4f^7 6p^+ J = 3$ ionization limit at 69509.2 cm^{-1}. The values of level energy (E) and width (Γ) of the $4f^7 6pnl$ autoionizing states of the Eu atom are obtained by fitting the experimental spectra to the Lorentz profile.

serial number	λ_3/nm	energy/cm^{-1}	Γ/cm^{-1}
1	460.80	60957.3	581.3
2	458.45	59547.4	432.7
3	458.94	59463.4	542.2
4	460.37	58999.9	598.1
5	458.62	58065.0	329.8
6	459.15	57871.1	557.4
7	460.25	57794.2	398.3
8	460.21	57766.6	410.1

Table 2 shows the level energies and the widths of $4f^7 6pnl$ autoionizing states converging to the $4f^7 6p^+ J = 3$ ionization limit at 69509.2 cm^{-1} of the Eu atom, which are obtained by fitting the experimental spectra to the Lorentz profile. As the width of an autoionizing state represents the total autoionization rate to all possible continuum states, it indicates the coupling strength of an autoionizing state with the underlying continua. In particular, two interesting phenomena can be found from Table 2: first, the autoionizing state located at 58999.9 cm^{-1} has the largest width (598 cm^{-1}), which represents the greatest autoionization rate in the energy region; second, the widths of the $4f^7 6pnl$ autoionizing Rydberg states have no apparent dependence on energy. To explain and understand the above phenomena two possibilities may be considered: a) these autoionizing states do not belong to the same autoionization series; b) they mix strongly with other $J = 3$ autoionization series.

In order to find out some differences between the states shown in Table 3, some comparisons are made. For instance, the widths of the $4f^7 6pnl$ autoionizing Rydberg states basically reduce with the increase of energy as expected. The only exceptions are found in the two states located at 62115.2 cm^{-1} and 61502.1 cm^{-1} respectively. The reason why they have a larger width than those states nearby is possibly due to the fact that they are heavily perturbed by other $J = 4$ autoionizing states belonging to other autoionization series.

Table 3. Autoionizing states converging to the $4f^7 6p^+$ $J = 4$ ionization limit at 69942.8 cm^{-1}. The values of energy level (E) and width (Γ) of the $4f^7 6pnl$ autoionizing states of the Eu atom are obtained by fitting the experimental spectra, similar to the ones shown in Figs. 4 and 5.

serial number	λ_3/nm	energy/cm^{-1}	Γ/cm^{-1}
1	440.32	62037.0	240.5
2	440.15	62248.4	247.2
3	441.36	62174.2	300.3
4	441.82	62115.2	498.9
5	442.63	61502.1	515.5
6	442.03	61434.4	405.1
7	442.58	61351.3	454.0
8	443.14	61493.5	552.9

It is also meaningful to make a comparison between Tables 2 and 3. Their similarity is apparent: both tables show obvious variations of the scaled widths indicating that both the $J = 3$ and $J = 4$ autoionization series are heavily perturbed. However, the difference between the two tables is also obvious: the widths of the $J = 4$ autoionization series basically reduce with the increase of energy, while the $J = 3$ $4f^7 6pnl$ autoionizing Rydberg states do not.

Above all, since an autoionizing state is a bound state that degenerates into many continuum states, its width represents the total autoionization rate to all possible continuum states, reflecting the coupling strength between an autoionizing state and the underlying continua. Since the autoionizing states considered in this work lie above the $4f^7 6s^+$ threshold, and are embedded in many continua, the configuration interaction may result in two effects for both $J = 3$ and

$J = 4$ $4f^7 6pnl$ autoionizing states: a) there are many complex structures on the spectra; b) the scaled autoionization rates may change significantly. These effects can be seen in their spectra shown in Figs. 4 and 5, or in Tables 2 and 3.

4. Conclusions

In this work, spectral information on highly excited states of the europium atom is investigated with a combination of resonant ionization spectroscopy and the technique of stepwise laser excitation. The bound Eu spectra with an odd parity in the region of 42400–43500 cm^{-1} are measured to obtain the positions and the intensities of 38 transitions, as well as their total angular momenta. Compared with the work reported in the relevant literature, the present work reveals 14 new states. Meanwhile, the autoionization spectra of atomic Eu, belonging to the $4f^7 6pnl$ configurations, are investigated by using the ICE scheme. Spectral information, such as their positions and widths, is obtained. Furthermore, a comparison between the $J = 3$ and $J = 4$ autoionizing states is made to explore the possible effects of the configuration interaction between autoionizing states and the underlying continua. Further study on the Eu $6p_{3/2}nl$ autoionizing states is in progress.

References

[1] Paspalakis E, Kylstra N J and Knight P L 1999 *Phys. Rev.* A **60** 642

[2] Lyras A and Bauchau H 1999 *Phys. Rev.* A **60** 4781

[3] Bhattacharyya S, Nakhate S G, Jayasekharan and Razvi M A N 2006 *Phys. Rev.* A **73** 062506

[4] Bhattacharyya S, Razvi M A N, Cohen S and Nakhate S G 2007 *Phys. Rev.* A **76** 012502

[5] Ogawa Y and Kujirai O 1999 *J. Phys. Soc. Jpn.* **68** 428

[6] Bíemont E, Garnir H P, Li Z B, Lokhnygin V, Palmeri P, Quinet P, Svanberg S, Wyart J F and Zhang Z G 2001 *J. Phys.* B **34** 1869

[7] Yi J H, Lee J M and Kong H J 1995 *Phys. Rev.* A **51** 3053

[8] Schulz J, Wernet Ph, Godehusen K, Muller R, Zimmermann P, Martins M and Sonntag B 2002 *J. Phys.* B **35** 907

[9] Nakhate S G, Razvi M A N, Connerade J P and Ahmad S A 2000 *J. Phys.* B: *At. Mol. Opt. Phys.* **33** 5191

[10] Bhattacharyya S, D'Souza R, Pushpa M and Razvi M A N 2003 *Spectrochimica Acta* Part B **58** 469

[11] Lu J, Dai C J, Xu Y F and Li S B 2001 *Chin. Phys. Lett.* **18** 1192

[12] Li S B, Dai C J, Sun W and Xue P 2001 *J. Phys.* B: *At. Mol. Opt. Phys.* **34** 2123

[13] Zhang Y, Dai C J and Li S B 2004 *J. Electron Spectrosc. Relat. Phenom.* **135** 63

[14] Li S B and Dai C J 2003 *J. Quantum Spectrosc. Radiat. Transfer* **77** 345

[15] Li S B and Dai C J 2007 *Chin. Phys.* **16** 382

[16] Li S B and Dai C J 2001 *J. Phys* B: *At. Mol. Opt. Phys.* **34** 981

[17] Nakhate S G, Razvi M A N, Bhale G L and Ahmad S A 1996 *J. Phys.* B: *At. Mol. Opt. Phys.* **29** 1439